Int J Earth Sci (Geol Rundsch) (2017) 106:1223–1238
DOI 10.1007/s00531-016-1314-3

ORIGINAL PAPER

Detrital zircon provenance analysis in the Zagros Orogen, SW Iran: implications for the amalgamation history of the Neo-Tethys

Zhiyong Zhang[1,2] · Wenjiao Xiao[1,3] · Mahmoud Reza Majidifard[4] · Rixiang Zhu[1] · Bo Wan[1,3] · Songjian Ao[1] · Ling Chen[1,3] · Mahnaz Rezaeian[5] · Rasoul Esmaeili[1]

Received: 29 October 2015 / Accepted: 24 February 2016 / Published online: 10 March 2016

Abstract The Zagros Orogen developed as a result of Arabia–Eurasia collision. New in situ detrital zircon U–Pb and Hf isotopic analyses from a Cenozoic sedimentary sequence in SW Iran are used to unravel the amalgamation history of Neo-Tethys. Data indicate that: (1) Paleocene and Eocene strata (58 and 45 Ma, respectively) were sourced from obducted ophiolite and Triassic volcanics, (2) Lower Miocene (~18 Ma) strata indicate mixed provenance from obducted ophiolite and Iranian magmatic rocks, (3) Mid to Upper Miocene sediments (~14 to 11.2 Ma) were mainly sourced from Sanandaj–Sirjan zone granitoids to the north, and (4) Lower Pliocene (~5 Ma) sediments mainly show Arabian age characteristics, with a minor Eurasian affinity component. Two hypotheses are outlined to highlight the key events: Hypothesis A, previously published by several workers, suggests that the sequence studied lay on the Arabia passive margin and that initial collision occurred prior to 18 Ma; Hypothesis B, modified from the Makran model, which is here preferred, suggests that Paleogene to Upper Miocene sediments were sourced from the northern Neo-Tethyan accretionary complex or Eurasia, and carry no input from Arabia, whereas the Lower Pliocene sample shows a mixed provenance from both Arabia and Eurasia, suggesting that collision occurred between ~11.2 and 5 Ma.

Keywords Neo-Tethys · Zagros Orogen · Arabia–Eurasia collision · Detrital zircon U–Pb geochronology · Hf isotopes

Electronic supplementary material The online version of this article (doi:10.1007/s00531-016-1314-3) contains supplementary material, which is available to authorized users.

✉ Zhiyong Zhang
zyzhang@mail.iggcas.ac.cn

✉ Wenjiao Xiao
wj-xiao@mail.iggcas.ac.cn

1 State Key Laboratory of Lithospheric Evolution, Institute of Geology and Geophysics, Chinese Academy of Sciences, Beijing 100029, China

2 School of Earth Sciences, The University of Melbourne, Parkville, VIC 3010, Australia

3 CAS Center for Excellence in Tibetan Plateau Earth Sciences, Beijing, China

4 Research Institute for Earth Sciences, Geological Survey of Iran, Tehran, Iran

5 Institute for Advanced Studies in Basic Sciences, Zanjan, Iran

Introduction

The NW–SE trending Zagros Orogen resulted from the collision between Arabia and Eurasia (Fig. 1). It consists of three different parallel structural units, which from NE to SW are: (1) the Urumieh–Dokhtar magmatic arc (UDMA); (2) the metamorphic and magmatic Sanandaj–Sirjan zone (SSZ); and (3) the Zagros fold and thrust belt (ZFTB). The so-called Main Zagros Thrust (MZT) is widely considered to represent the suture between the Arabian and Eurasian plates (Agard et al. 2011; Alavi 1994). The SSZ is generally regarded to be located on the southern active margin of the Eurasian plate, which was thrust southwestward over the ZFTB (Homke et al. 2009). The ZFTB is characterized by well-developed open folds, which involve the entire 12–14 km-thick sedimentary cover of the Zagros Basin.

The Zagros Orogen is separated from the Makran region by the Oman Line (Mouthereau et al. 2012; Talebian and Jackson 2004). New field observations and geochemical and geochronological data indicate affiliation

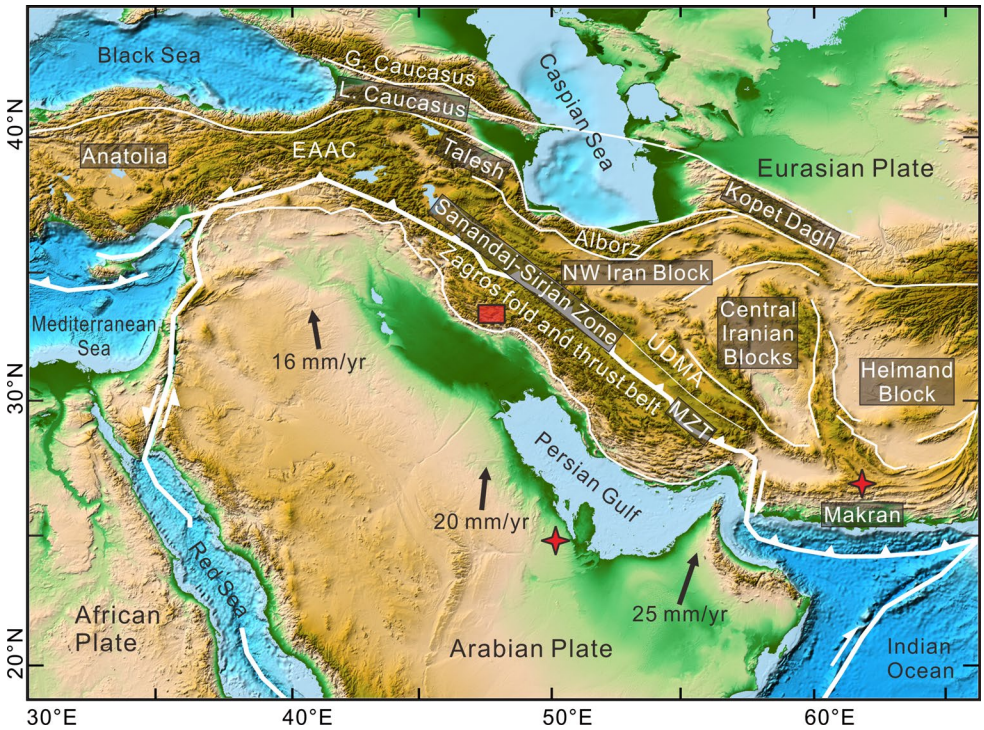

Fig. 1 Tectonic setting of the Arabia–Eurasia collision zone (Austermann and Iaffaldano 2013; Homke et al. 2009; Mouthereau et al. 2012). The *background image* is from ETOPO1 Global Relief Model (National Geophysical Data Center, NOAA, http://ngdc.noaa.gov/mgg/global/). Velocities of Arabia with respect to Eurasia (ArRajehi et al. 2010). *EAAC* East Anatolian Accretionary Complex. The *two stars* indicate the locations of Aeolian dune samples from Arabia and Oligocene–Miocene sandstone samples from Makran (Carter et al. 2010; Garzanti et al. 2013), detrital zircon U–Pb data of these samples are cited for comparison in Fig. 9. *Red rectangle* shows the study area. See Fig. 3 for more detailed geological information

of North Makran granitoids to plutons of the Sanandaj-Sirjan Zone. This defines a narrow, NW–SE striking and nearly 2000 km long belt of Jurassic intrusions, indicating the same tectonic regime along the southern Iranian continental margin at that time (Hunziker et al. 2015). Compared to the southward retrogression of the Makran trench and the accretionary sediment wedge during the consumption of oceanic crust in the Cenozoic, Arabia collided with Eurasia forming the Zagros Orogen as a continental convergent plate boundary. The difference between the Zagros and Makran is probably due to the morphological features of plates. The fundamental problem and current debate concerning the Zagros Orogen relates to the amalgamation history of Neo-Tethys, and especially the age of final continental collision (Dewey et al. 1986; Gavillot et al. 2010; Hempton 1987; Şengör and Natal'in 1996; Yin 2010). The time of the Arabia–Eurasia collision has previously been proposed to vary from late Cretaceous to Pliocene (Alavi 1994; Berberian and King 1981; Dercourt et al. 1986; Dewey et al. 1973, 1986; Hempton 1987; Şengör and Natal'in 1996; Stoneley 1981; Talebian and Jackson 2004), although recent publications suggest that collision was between 38 and 20 Ma (Fig. 2) (Agard et al. 2005, 2011; Allen and Armstrong 2008; Ballato et al. 2011; Fakhari et al. 2008; Khadivi et al. 2012; McQuarrie and van Hinsbergen 2013; Saura et al. 2015). Meanwhile, property of the Zagros sedimentary rocks, and position of the Neo-Tethys suture zone also remain controversial (Farhoudi 1978; Hunziker et al. 2015).

Comparison between U–Pb zircon probability density plots of detrital sediments and potential source terranes is now widely used to reveal the history of ancient plate margins and to interpret linkages between sediment sources and sinks (Cawood et al. 2013; Gehrels 2014). Detrital zircon age spectra are a powerful tool to help clarify such links between long-dispersed blocks, to constrain terrane amalgamation events, to resolve complex relationships between rock units within suture zones and to determine the tectonic setting of basins (Cawood et al. 2013; Gehrels 2014).

Previously, only one detrital zircon U–Pb study in Iran provided data from a single Miocene sandstone sample in north-central Iran (Horton et al. 2008). No systematic results have been reported for Cenozoic deposits from the Zagros Orogen. In order to provide constraints on the amalgamation history of Neo-Tethys and to resolve the controversy regarding the timing of the Arabia–Eurasia collision, we have conducted a systematic U–Pb geochronological study and Lu–Hf isotopic analyses of detrital zircons in Cenozoic deposits in the Lurestan Province of SW Iran (Fig. 3).

Geological setting

In Lurestan the Meso-Cenozoic stratigraphic column consists of the following units, from bottom to top: Mesozoic carbonate units, basinal calcareous Gurpi–Pabdeh Formation, Amiran slope deposits, Taleh Zang mixed

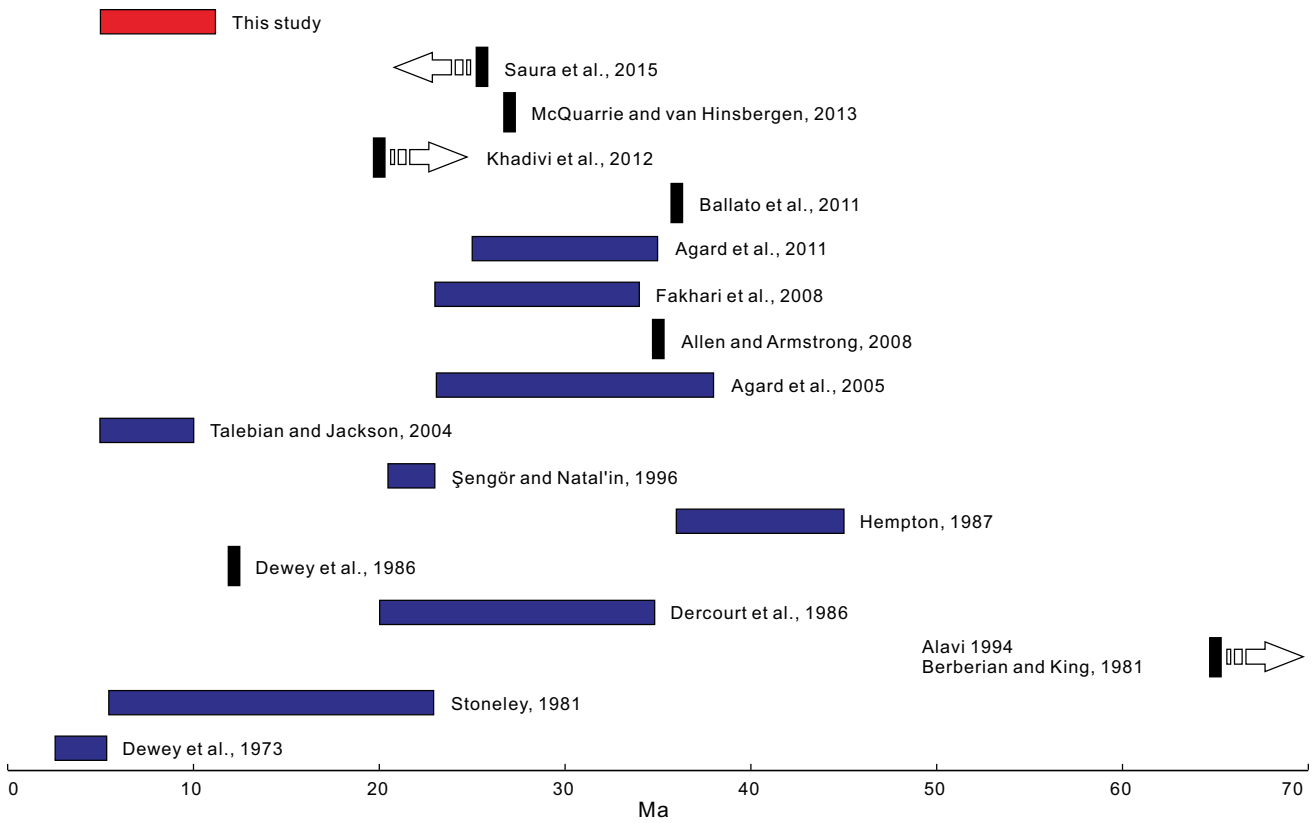

Fig. 2 Summary of published ages for onset of continental collision between Arabia and Eurasia

clastic-carbonate platforms, continental Kashkan red beds, Shahbazan–Asmari shallow-marine carbonate platform, evaporitic Gachsaran Formation, and siliciclastic Agha Jari and Bakhtyari Formations (Fig. 4) (Homke et al. 2004, 2009; Saura et al. 2011, 2015). The Gurpi Formation is composed of decimeter-scale beds of gray marl and fine-grained limestones. The Amiran Formation grades laterally into the Pabdeh Formation (James and Wynd 1965). The red conglomeratic Kashkan Formation and the shallow-water carbonate and detrital Taleh Zang Formation are succeeded by the regional shallow-marine platforms of the Shahbazan and Asmari formations (Homke et al. 2009; Saura et al. 2011). The evaporitic Gachsaran Formation, overlying the Asmari limestones, records a regression from marine to nonmarine conditions (Emami 2008). The fluvial Agha Jari Formation is in turn overlain by conglomerates of the Bakhtyari Formation, which form the uppermost sedimentary unit (Emami 2008; Homke et al. 2004; James and Wynd 1965).

Methods

Six representative samples were collected from different stratigraphic horizons along a well-exposed section in Lurestan Province, SW Iran. Relative stratigraphic positions are shown in Fig. 4. Photographs of outcrops are shown in Fig. 5 and microphotographs of samples in Fig. 6. Zircon crystals were separated from 3 to 4 kg rock samples using conventional heavy liquid and magnetic techniques. Individual zircon grains were handpicked randomly, mounted in epoxy resin and then polished to expose their internal surfaces. Cathodoluminescence (CL) images of zircons were prepared in order to identify internal structures and choose potential target sites for U–Pb and Hf isotopic analyses (Fig. 7).

Both zircon U–Pb and Hf analyses were carried out at the State Key Laboratory of Lithospheric Evolution, Institute of Geology and Geophysics, Chinese Academy of Sciences.

Zircon U–Pb dating was performed on an Agilent 7500a Q–ICP–MS equipped with a 193-nm excimer ArF laser ablation system (Geolas Plus), following procedures described in Wu et al. (2010). A spot diameter of 44 µm was used. $^{207}Pb/^{206}Pb$ and $^{206}Pb/^{238}U$ ratios were calculated using the GLITTER program (GEMOC, Macquarie University), which was then corrected using Harvard zircon 91500 as an external standard. Common Pb corrections were made following the method described by

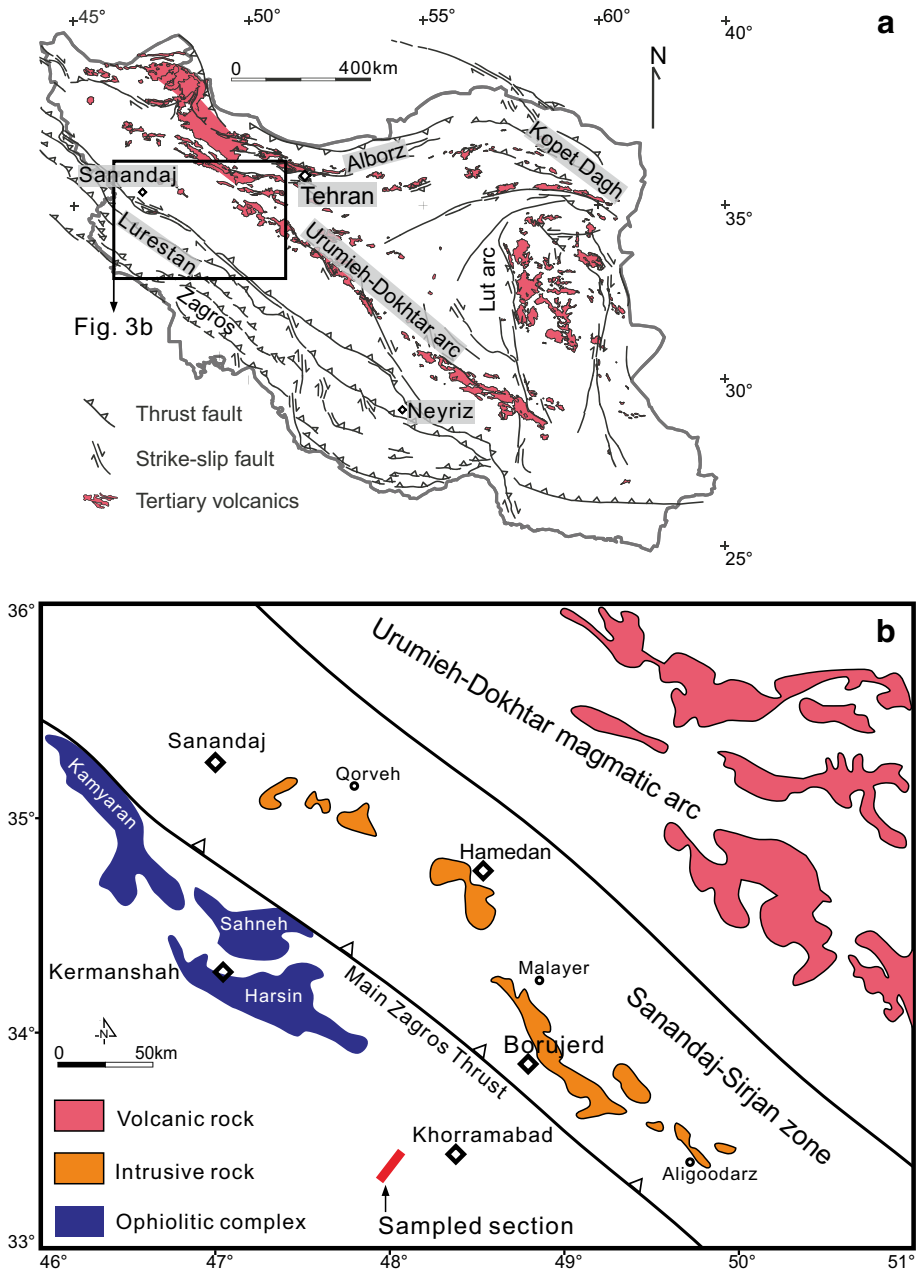

Fig. 3 **a** Distribution of Tertiary volcanic rocks and major faults in Iran (Verdel et al. 2011). *Rectangle outlines* the location of the Lurestan Province and **b**. **b** Simplified geological map showing the relative location of the sampled section, the Kermanshah ophiolite and plutons in the Sanandaj–Sirjan zone

Andersen (2002). The zircon U–Pb data are listed in Online Resource 1, concordia diagrams are shown in Fig. 8, and density plots are shown in Fig. 9. For ages <1200 Ma, the $^{206}Pb/^{238}U$ age is used, whereas the $^{207}Pb/^{206}Pb$ age is used for zircons older than 1200 Ma. For statistical purposes, zircons with concordance >90 and <110 % are considered as usable.

Zircon Hf isotopic analyses were attained using a Neptune MC–ICPMS equipped with a 193-nm excimer ArF laser ablation system (Geolas Plus). Details on instrumental conditions and data acquisition can be found in Wu et al. (2006). Hf isotopic analyses were carried out on the same sites as the U–Pb analyses with the same or a slightly larger laser beam size. The average $^{176}Hf/^{177}Hf$ ratio of standard zircon Mud Tank is 0.282504 ± 5, which is in accordance with the reported values (Woodhead and Hergt 2005); therefore, an external correction has not been applied to the analytical results. The Hf isotopic data are listed in Online Resource 2, $\varepsilon_{Hf}(t)$ versus U–Pb age plots are displayed in Fig. 10.

Results

The stratigraphic ages of the above rock units are well constrained by magnetostratigraphy, biostratigraphy and

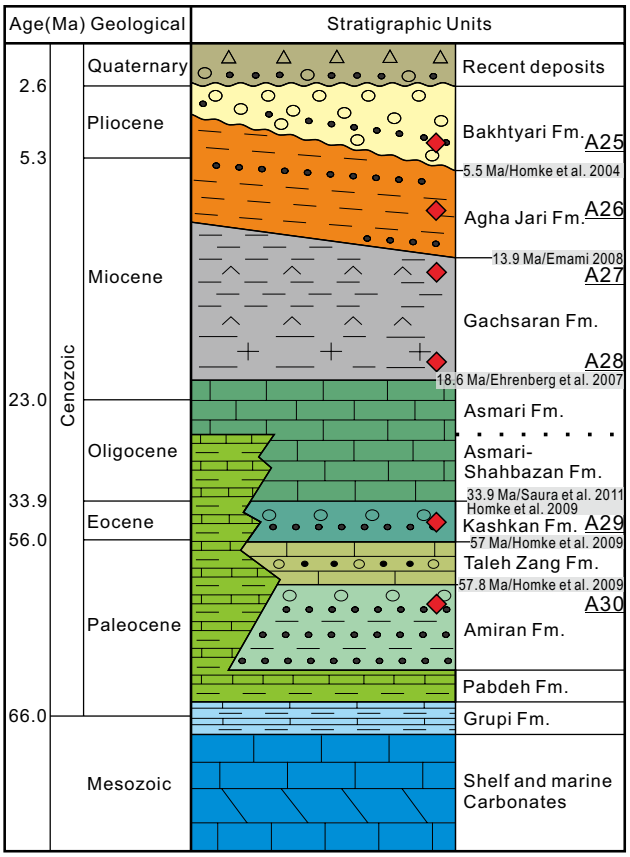

Fig. 4 Stratigraphic chart of the Zagros (Gavillot et al. 2010; Homke et al. 2009). Age boundaries follow the geologic time scale in Gradstein et al. (2012). Stratigraphic horizons of the samples dated are indicated by *red diamonds*

strontium isotope dating (Ehrenberg et al. 2007; Emami 2008; Homke et al. 2004, 2009; Saura et al. 2011). According to magnetostratigraphic data, the contact between the Agha Jari Formation and overlying sediments is 5.5 Ma (Homke et al. 2004), the Gachsaran–Agha Jari contact is dated at 13.9 Ma (Emami 2008), and the age of the base-Gachsaran is estimated at 18.6 Ma (Ehrenberg et al. 2007). The depositional ages of sample A25, A26, A27 and A28 are calculated to be at ca. 5, 11.2, 14 and 18 Ma, respectively. On the basis of the biostratigraphic, magnetostratigraphic and strontium isotope dating data (Homke et al. 2009; Saura et al. 2011), the depositional ages of samples A29 and A30 are at ca. 45 and 58 Ma, respectively.

Sample A25, a yellowish gray sandstone, was collected from the Bakhtyari Formation, in which the zircons are variable in size, and most are fine and stubby to round in shape. One hundred and twenty spots were analyzed from which 111 ages were used. Most ages fall between Early Cambrian and Neo-Proterozoic with the main peak at 621 Ma. The two youngest $^{206}Pb/^{238}U$ ages are 40 ± 4 and 41 ± 2 Ma. The $\varepsilon_{Hf}(t)$ values have a very wide range from −23.6 to +18.0 with $\varepsilon_{Hf}(t)$ versus U–Pb age diagram showing dispersive pattern (Fig. 10a). Most zircons with ages less than 350 Ma show positive $\varepsilon_{Hf}(t)$ values (Fig. 10b), whereas zircons with ages between 500 and 1100 Ma yield comparable negative and positive $\varepsilon_{Hf}(t)$ values (Fig. 10a).

Sample A26 was taken from a fine-grained sandstone in the middle of the Agha Jari Formation, which comprises brown to red silty-clay layers intercalated with gray to brown sandstone beds. Zircons from the sample are stubby with an average length of ca. 100 μm, some of which show oscillatory zoning under CL. 120 spots were analyzed, of which 114 ages were usable. The majority of ages are Phanerozoic with the main peak at 177 Ma. The youngest $^{206}Pb/^{238}U$ ages are 141 ± 5 and 142 ± 8 Ma. The $\varepsilon_{Hf}(t)$ values also show a very wide range from −29.0 to +15.1 (Fig. 10a). However, 27 zircons have uniform $\varepsilon_{Hf}(t)$ values between −2.0 and +2.8 at 160–200 Ma except one grain with a $\varepsilon_{Hf}(t)$ value of −4.9 (Fig. 10b).

Sample A27 was collected from purple medium-grained sandstones of the uppermost Gachsaran Formation in which the zircons are small, subhedral to euhedral and most show oscillatory zoning under CL. Among the 120 zircon analyses, 111 concordant analyses show a large range of ages from 28 ± 3 to 2937 ± 25 Ma, with a more complex age population than in the other samples. The weighted average age of the six youngest ages is 33.4 ± 3.5 Ma. The major peak is at 172 Ma with two minor peaks at 37 and 1870 Ma. Sample A27 has a wide range of $\varepsilon_{Hf}(t)$ values from −27.1 to +13.0 (Fig. 10a). The zircons have $\varepsilon_{Hf}(t)$ values between −0.4 and +8.0 at 28–40 Ma. Within the age cluster between 150 and 190 Ma, 16 zircons have $\varepsilon_{Hf}(t)$ values ranging from −1.9 to +3.6 except one zircon $\varepsilon_{Hf}(t)$ value of −11.6 (Fig. 10b).

Sample A28, a light gray fine-grained sandy limestone, was collected from a thin interlayer in the lowermost Gachsaran Formation in which the zircons are variable in size, and most crystals are euhedral. Ninety useable zircon U–Pb analyses were obtained from 100 analyses. The resultant zircon age pattern differs from the age distribution found in the other samples. The major peak is at 58 Ma with two minor peaks at 107 and 284 Ma. The youngest grain age is 29 ± 3 Ma, and the weighted average age of the five youngest ages is 36 ± 5 Ma. The $\varepsilon_{Hf}(t)$ values of this sample range from −22.6 to +14.4, with the $\varepsilon_{Hf}(t)$ versus U–Pb age plot showing a dispersive pattern (Fig. 10a). Of the 21 zircons from the youngest group (29–72 Ma), 19 have $\varepsilon_{Hf}(t)$ values between −0.4 and +5.0 except another two yielding $\varepsilon_{Hf}(t)$ values of −3.0 (Fig. 10b).

Sample A29, a red coarse-grained sandstone, was taken from a thin layer in the middle of the Kashkan Formation, in which the zircons are euhedral and large. Seventy useable zircon analyses were obtained from 74 analyses. The major peak is at 101 Ma with a minor peak at 244 Ma. The

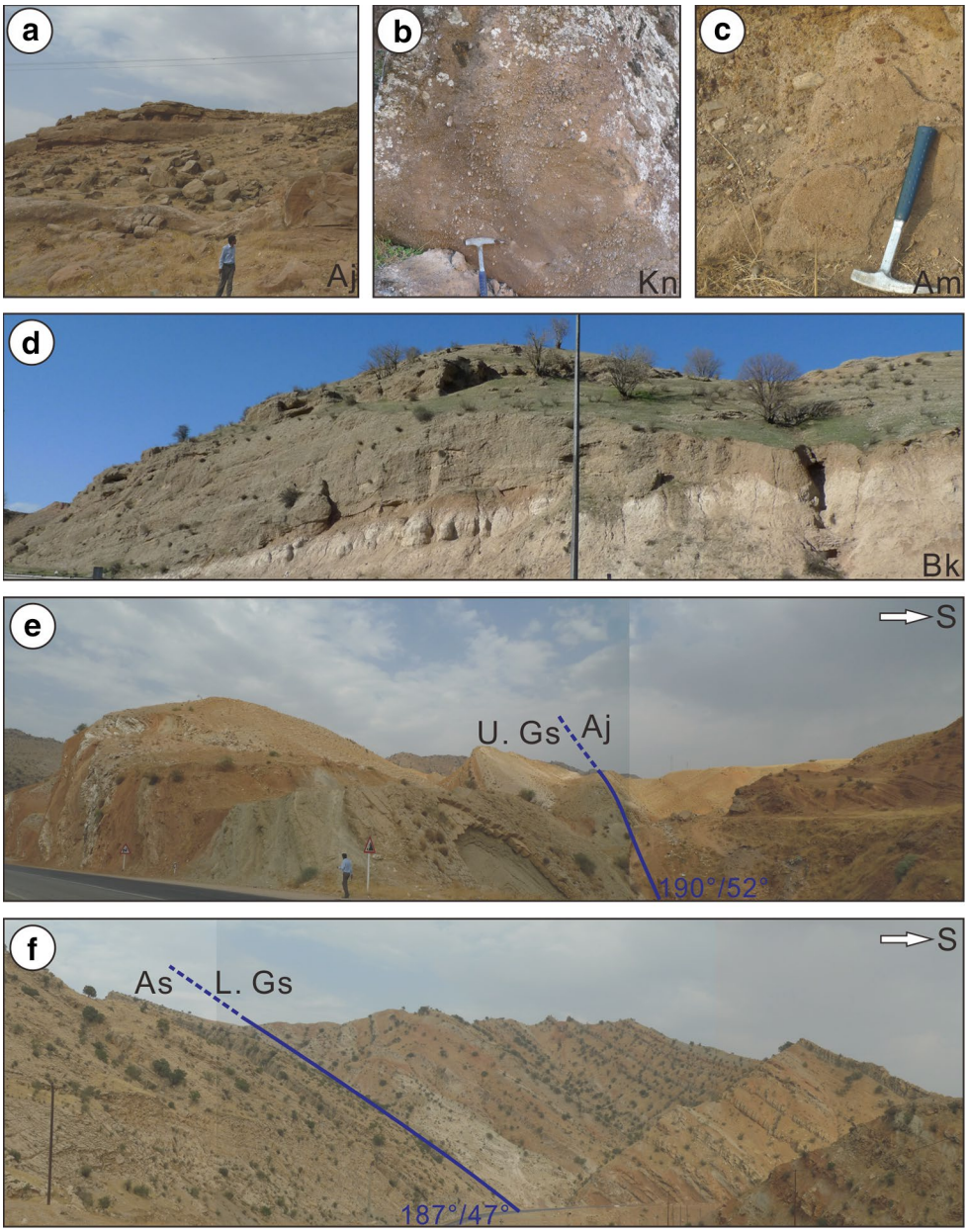

Fig. 5 Photographs of outcrops for sampled formations from the Zagros Orogen in Lurestan Province, SW Iran. **a** Horizontal layer of Agha Jari Formation (Aj) in the core of Afrineh syncline. **b** Kashkan Formation (Kn). **c** Amiran Formation (Am). **d** Bakhtyari Formation (Bk). **e** 190°/52° is dip direction and dip angle of stratigraphic boundary between Agha Jari Formation and Upper Gachsaran Formation (U. Gs). **f** Stratigraphic boundary between Lower Gachsaran Formation (L. Gs) and Asmari Formation (As) has a dip direction of 187° and dip angle of 47°

two youngest $^{206}Pb/^{238}U$ ages are 82 ± 9 and 83 ± 3 Ma. Most of the zircons show high $^{176}Hf/^{177}Hf$ ratios and positive $\varepsilon_{Hf}(t)$ values (Fig. 10a). The zircon $\varepsilon_{Hf}(t)$ values at ca. 244 Ma are higher than those at ca. 101 Ma (Fig. 10b).

Sample A30, a gray coarse-grained sandstone, was collected from the upper part of the Amiran Formation. Zircons here are similar to those in A29, except that a few are fragmented. One hundred and three usable zircon analyses were obtained from 119 analyses with two main peaks at ca. 100 and 245 Ma. The younger peak displays a bimodal pattern with two secondary peaks at 94 and 105 Ma. The two youngest $^{206}Pb/^{238}U$ ages are 65 ± 4 and 72 ± 4 Ma. Similar to sample A29, most of the zircons here show high $^{176}Hf/^{177}Hf$ isotopic ratios and positive $\varepsilon_{Hf}(t)$ values (Fig. 10a). The zircon $\varepsilon_{Hf}(t)$ values at ca. 245 Ma range between −2.6 and +19.5, while zircons at ca. 100 Ma have $\varepsilon_{Hf}(t)$ values ranging between +0.8 and +13.2 (Fig. 10b).

It is generally accepted that the youngest concordant detrital zircon ages can be used to constrain the maximum depositional age (Cawood et al. 1999). The youngest concordant zircon ages of samples A27, A28 and A30 are ca. 10 Ma older than the depositional age, whereas the youngest concordant zircon ages of samples A25, A26 and A29 are considerably older than their depositional ages.

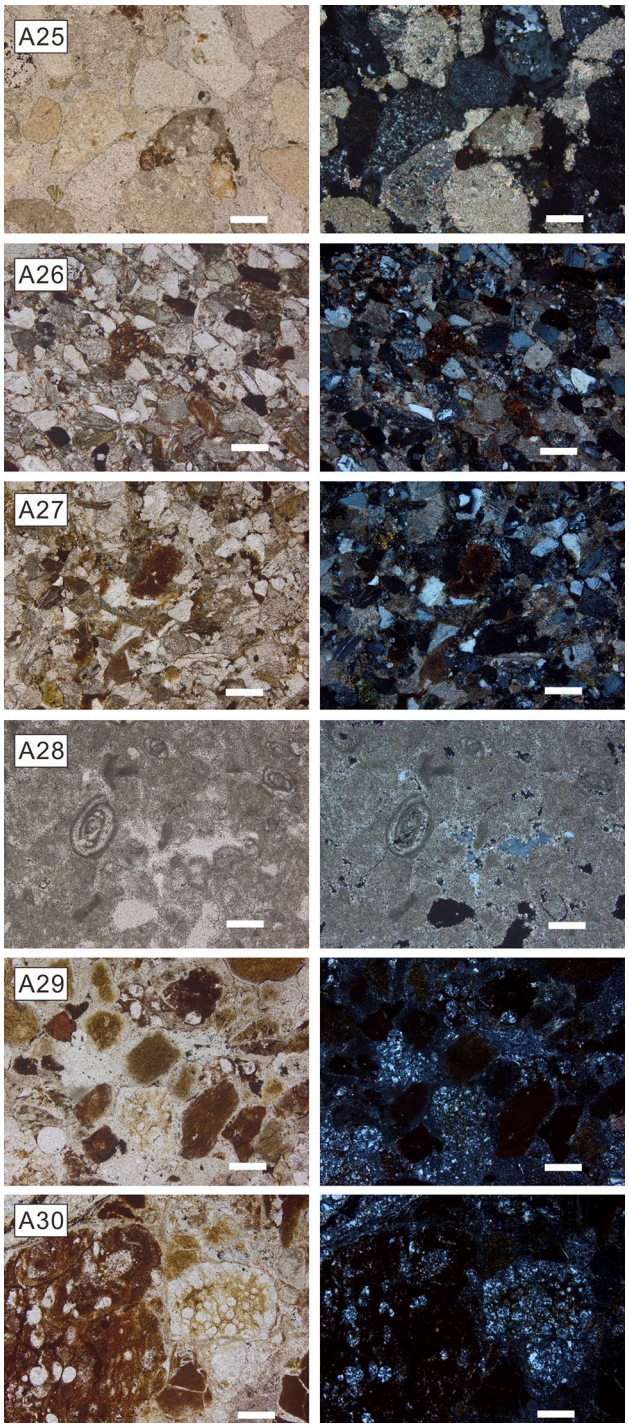

Fig. 6 Microphotographs (*plane* and *crossed polarized light*) of the samples. Main composition: chert and round carbonate detritus (A25); quartz, feldspar, carbonate and limonite (A27, A27); foraminifer fossils (having experienced carbonate metasomatism), embayed quartz (indicating continental detrital character) (A28); radiolarian chert (A29, A30). *White scale* shown in all photos is 200 μm

Discussion

Provenance analysis

Provenance of samples A29 and A30

Samples A29 and A30 share the same dominant age population ranging from 65 to 300 Ma (Fig. 9). Comparison between detrital zircon U–Pb ages of the two samples reveals a close similarity, suggesting a common source. Regional-scale obduction of the Neo-Tethyan oceanic lithosphere is known to have taken place in the period ca. 100–65 Ma (Agard et al. 2005, 2011; Searle and Cox 1999; Whitechurch et al. 2013). However, much of the Neo-Tethyan ophiolites has either been eroded and/or later buried, except the Semail ophiolite in the Oman Mountains (Agard et al. 2011; Searle and Cox 1999). Further, a few obduction-related ophiolite remnants are found in Kermanshah and Neyriz along the MZT (Ao et al. 2016, in press; Delaloye and Desmons 1980; Ghazi and Hassanipak 1999). Therefore, the preferred provenance of samples A29 and A30 is the presumed eroded and/or buried ophiolites near Khorramabad. This implies that the erosion of obducted Neo-Tethyan ophiolite likely fed detrital basins in the study area. This deduction is also supported by the petrography of samples A29 and A30, which indicates that the Amiran and Kashkan formations contain ophiolitic detritus including abundant radiolarian chert fragments and a few serpentine grains. Moreover, the proposed source of the Neo-Tethyan ophiolite to the north is consistent with measured S to SSW paleocurrent directions (Homke et al. 2009). As for the age correlation, the age of the Harsin/Sahneh ophiolite (part of the Kermanshah ophiolite) is estimated at 86.3 ± 7.8 and 81.4 ± 3.8 Ma by $^{40}K/^{39}Ar$ dating (Delaloye and Desmons 1980). The zircon U–Pb age should be theoretically more or less older than the $^{40}K/^{39}Ar$ age due to the higher closure temperature of the U–Pb isotopic system. However, new precise zircon U–Pb data indicate that the younger part of the Kermanshah ophiolite formed at 35.7 ± 0.5 Ma and the older part at 79.3 ± 0.9 Ma (Ao et al. 2016, in press). This confirms that the eroded ophiolite is even older than the remnant Kermanshah ophiolite. This idea is supported by detrital zircon U–Pb data from Cenozoic sediments of the Makran accretionary prism in southeastern Iran, which reveal a main peak at ca. 104 Ma (Carter et al. 2010). So the younger peaks at ca. 100 Ma of samples A29 and A30 are consistent with ages of the Neo-Tethyan ophiolite (Moghadam et al. 2013; Searle

Fig. 7 Representative cathodoluminescence (CL) images of zircons from Cenozoic deposits in Lurestan Province, SW Iran. *Circles* indicate positions of laser spots for age and Hf isotopic analyses. Analytical number, apparent age (*underlined*), and $\varepsilon_{Hf}(t)$ value (in *italics*) are denoted

and Cox 1999). Meanwhile, zircons dated at ca. 100 Ma from samples A29 and A30 have positive $\varepsilon_{Hf}(t)$ values, indicating a juvenile magma source. This is in accordance with zircon $\varepsilon_{Hf}(t)$ values of the Neo-Tethyan Kermanshah ophiolite ranging between +1.1 and +12.1 at ~80 Ma (Ao et al. 2016, in press). The Neo-Tethys between Arabia and Eurasia began rifting during the early Permian and separated the Cimmerian continent from Gondwanaland. Continued stretching and abundant volcanism occurred in the early to middle Triassic, coincides with the peaks at ca. 245 Ma of samples A29 and A30 (Berberian and King 1981; Mohajjel et al. 2003; Searle and Cox 1999; Şengör et al. 1988; Şengör and Natal'in 1996; Stampfli and Borel 2002). The wide range of zircon $\varepsilon_{Hf}(t)$ values at ca. 245 Ma maybe suggest isotopic inhomogeneity of source rocks, probably owing to different degrees of contamination from ancient crust.

Provenance of sample A28

The age distribution pattern of sample A28 is characterized by a mixed provenance from a Neo-Tethyan obduction-related ophiolite (or recycled underlying the Amiran–Taleh Zang–Kashkan Formations) and Iranian magmatic rocks (Eurasian affinity). The major peak at ca. 58 Ma is correlated with the late Paleocene–Eocene magmatic "flare-up" in Iran (Chiu et al. 2013; Verdel et al. 2011). Moreover, the Early Tertiary Magmatic Domain (ETMD) is proposed to define this magmatic activity (Agard et al. 2011). The ETMD is well exposed near the study area, having formed in Paleocene–Early Eocene time on the Eurasian side of Neo-Tethys (to the south of the SSZ), probably as a result of slab break-off (Agard et al. 2011; Whitechurch et al. 2013). The younger minor peak at 107 Ma is consistent with the major peaks of samples A29 and A30, while the older minor

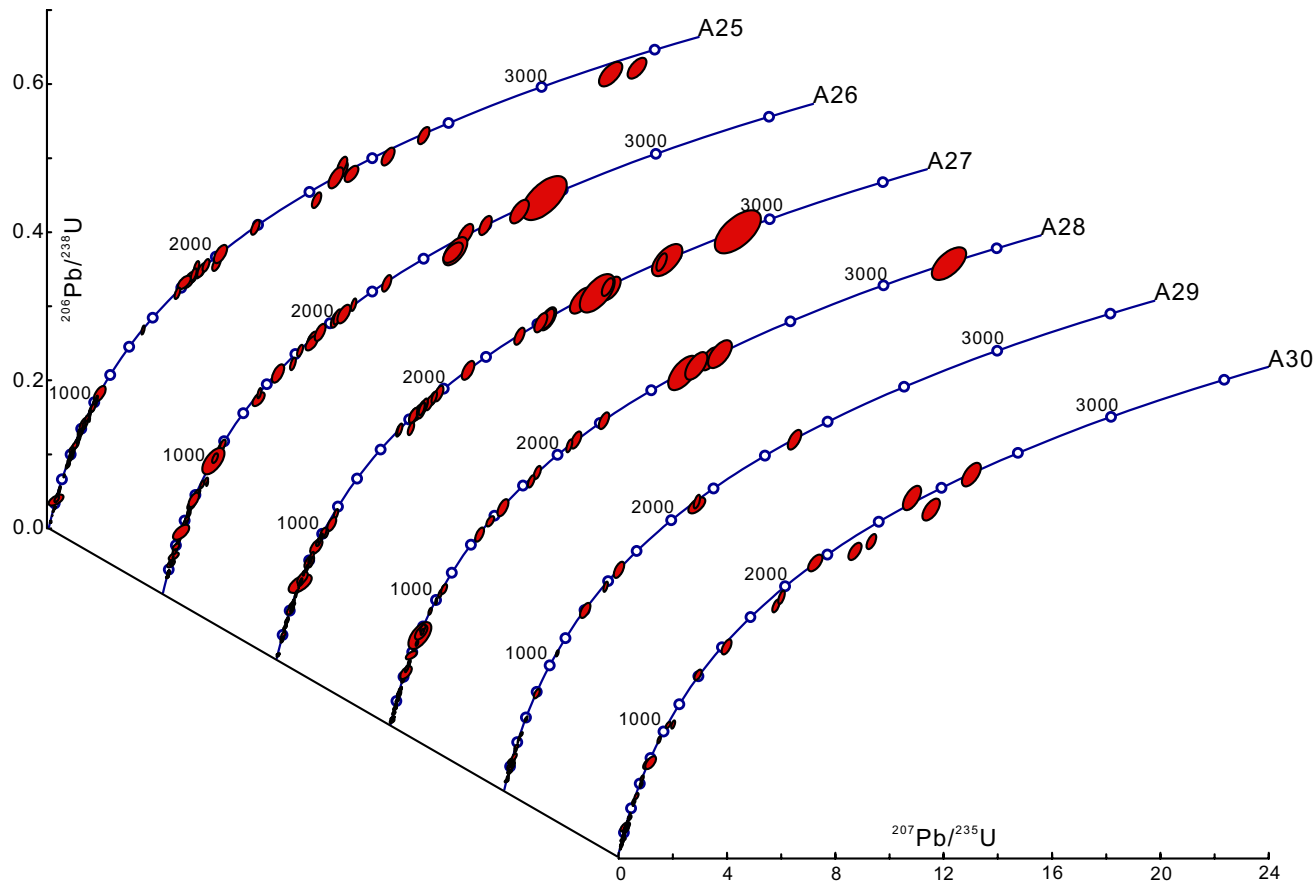

Fig. 8 Compound U–Pb concordia diagrams of samples collected from Cenozoic deposits in Lurestan Province, SW Iran. Ages are in Ma and ellipses show 1σ errors. Highly discordant analyses are not included

peak at 284 Ma might be related to a metamorphic complex in Central Iran (Bagheri and Stampfli 2008). The evidence for mixed provenances in this sample is supported by multiple age groups and various zircon $\varepsilon_{Hf}(t)$ values.

Provenance of samples A26 and A27

The SSZ shows two characteristic peaks of magmatism at ca. 40 Ma and ca. 170 Ma (Fig. 9) (Chiu et al. 2013). The strong correlation between the timing of magmatism in the SSZ and the age peaks of samples A26 and A27 lead us to conclude that the SSZ is the main provenance of the uppermost Gachsaran Formation and the Agha Jari Formation. The detailed source areas are probably connected upstream to the Aligoodarz granitoid, the Malayer–Borujerd granitoid complex and the Alvand pluton (near Hamedan). Zircon U–Pb analyses of the Aligoodarz granitoid yield a crystallization age of ca. 165 Ma (Esna-Ashari et al. 2012). Most samples taken from the Malayer–Borujerd granitoid complex yield zircon U–Pb ages of ca. 170 Ma, while one sample collected from a small outcrop yields a zircon U–Pb age of 35 Ma (Ahadnejad et al. 2011; Ahmadi Khalaji et al. 2007; Mahmoudi et al. 2011). The zircon U–Pb age of the Alvand pluton is ca. 165 Ma (Chiu et al. 2013; Mahmoudi et al. 2011; Shahbazi et al. 2010). Therefore, due to their similar age distribution patterns, all these magmatic rocks from the SSZ are proposed to be the principal source area. This view is in agreement with westward paleocurrent directions (Emami 2008). Zircon U–Pb geochronological studies around Sanandaj suggest that there were three magmatic events at 157–144, 55 and 37 Ma (Azizi et al. 2011a, b; Mahmoudi et al. 2011). These plutons may provide a limited contribution to samples A26 and A27 as a distant igneous source. Furthermore, Middle to Late Jurassic I-type granitoids in the SSZ show a heterogeneous isotopic affinity with variable zircon $\varepsilon_{Hf}(t)$ values between −5 and +12 (Chiu 2013). It fits well with zircon $\varepsilon_{Hf}(t)$ values at ca. 175 Ma of samples A26 and A27. Overall, the sediment provenance of samples A26 and A27 is therefore well constrained by recent publications and our data.

Provenance of sample A25

Detrital zircon age spectra of sample A25 are more complicated than those of other samples. Zircons with

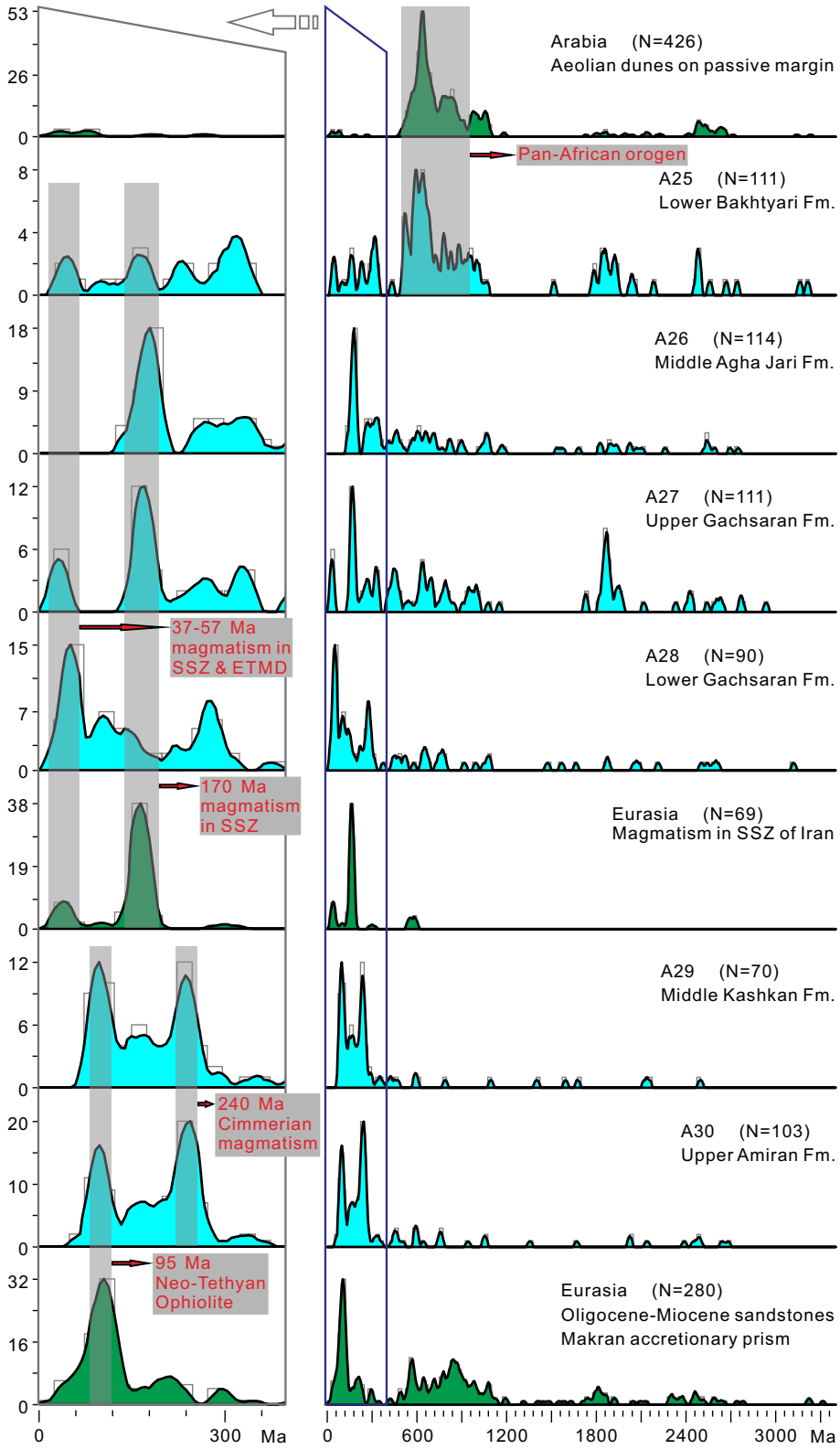

Fig. 9 Detrital zircon geochronology of Cenozoic samples from the Zagros Orogen in Lurestan Province, SW Iran. U–Pb age spectra plotted as histograms and kernel density estimates (Vermeesch 2012). *Horizontal axis* shows age in Ma, vertical axis the counts of the histogram. N = number of concordant ages. The age distribution patterns of Cenozoic sedimentary rocks from Makran (Carter et al. 2010), Aeolian dune samples from Arabia (Garzanti et al. 2013), and published data from SSZ (Ahadnejad et al. 2011; Ahmadi Khalaji et al. 2007; Azizi et al. 2011a, b; Carter et al. 2010; Chiu et al. 2013; Esna-Ashari et al. 2012; Garzanti et al. 2013; Mahmoudi et al. 2011; Shahbazi et al. 2010) are also shown in *green* for comparison

a Pan-African (950–500 Ma) signature account for up to sixty percent of the dated samples. A comparison of provenance can be made between our results and those from Arabia (Fig. 9). Samples of beach sands from the Arabian passive continental margin are dominated by Pan-African sources with subordinate contribution of zircons at ca. 1.0 and 2.5 Ga (Garzanti et al. 2013). The characteristics of sample A25 are consistent with

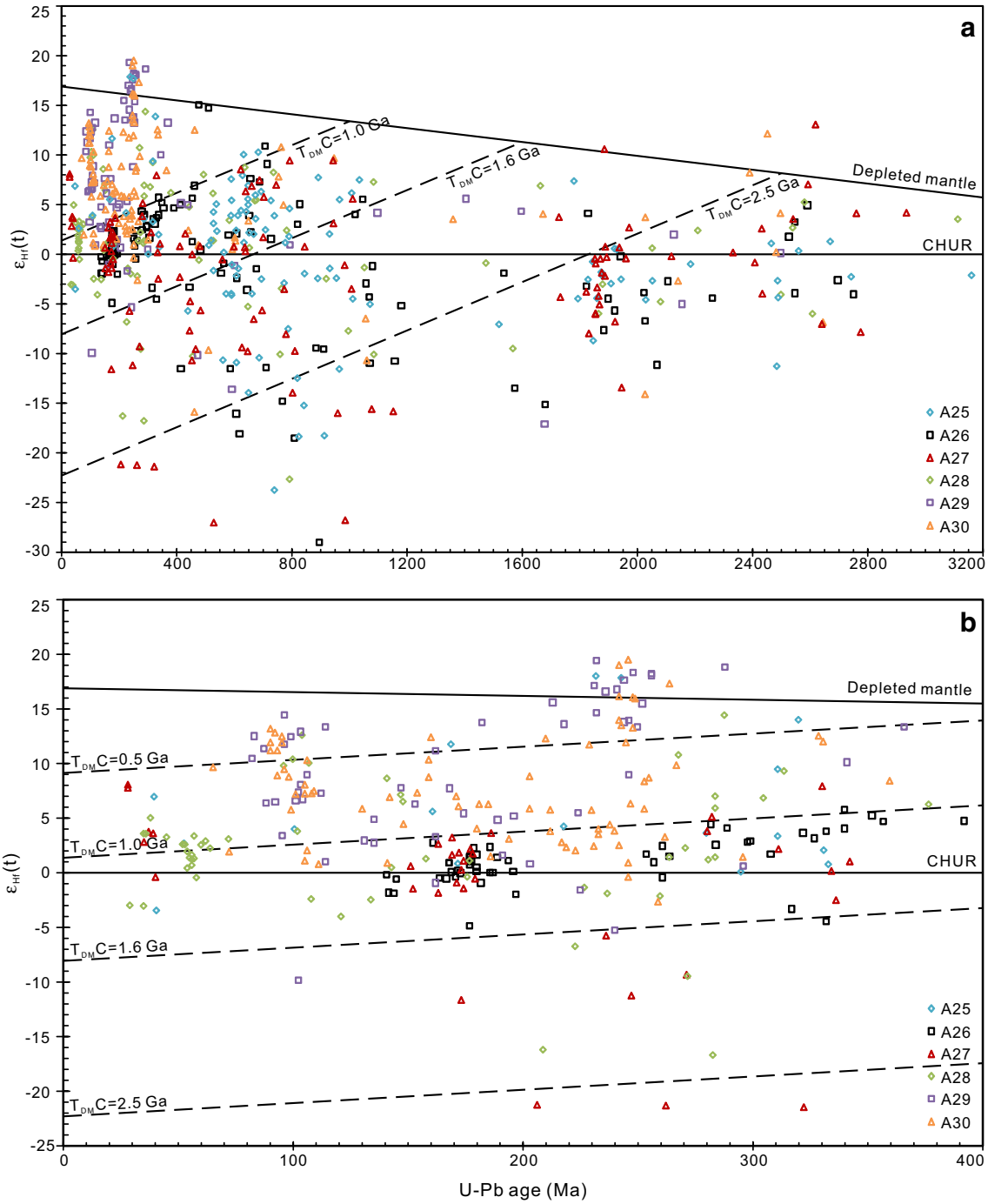

Fig. 10 $\varepsilon_{Hf}(t)$ values plotted against U–Pb ages for detrital zircon grains from Cenozoic deposits in Lurestan Province, SW Iran. Zircon U–Pb ages range from 0 to 3200 Ma along the *x*-axis in **a**, but range from 0 to 400 Ma in **b**

derivation from Arabia because its age distribution pattern is very similar to that of Arabian samples, while the age distribution patterns of the other five samples differ markedly from that of Arabian samples. Zircons from sample A25 with ages between 500 and 1100 Ma exhibit Hf isotopic data, which is analogous to published Hf data from U–Pb dated detrital zircons of the Cambrian–Ordovician sandstone which tops the juvenile Neoproterozoic basement of the Arabian-Nubian Shield in Israel and Jordan (Morag et al. 2011). Besides this age group, sample A25 also shows some small multiple age groups with Eurasian affinity.

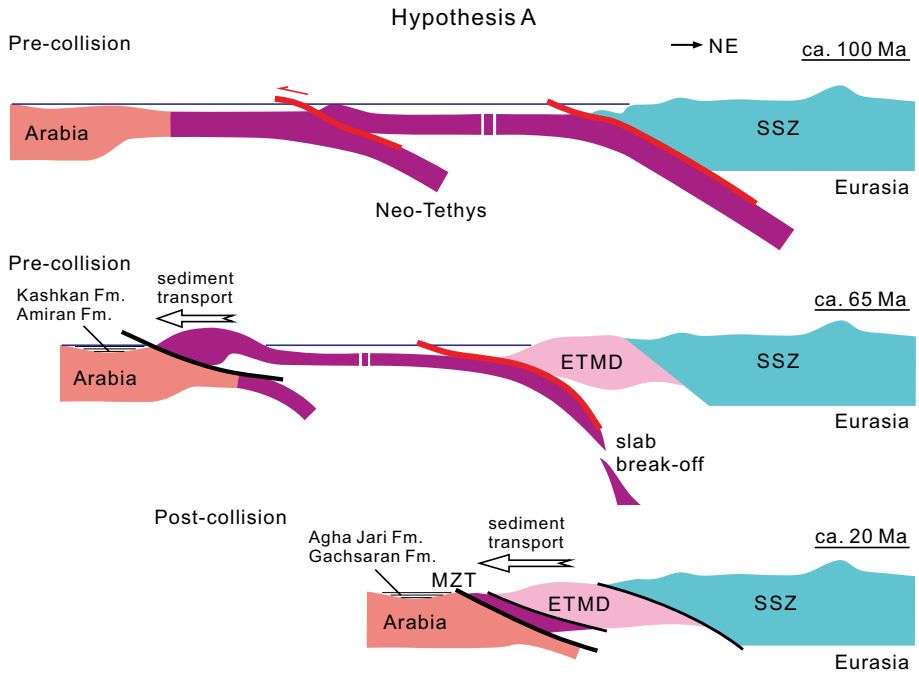

Fig. 11 Simplified tectonic evolution model (Hypothesis A) showing the amalgamation history of the Neo-Tethys indicating convergence between Arabia and Iran (Eurasia) since Late Cretaceous time (Agard et al. 2005, 2011; Whitechurch et al. 2013; Wrobel-Daveau et al. 2010). *Blue horizontal lines* indicate sea level. *Dark purple blocks* indicate Neo-Tethys ocean relict. *Red lines* represent incipient thrusts, while *black lines* represent obduction thrusts. See text for details

Tectonic implications

Our study presents detrital zircon U–Pb and Hf isotopic data from Cenozoic deposits from the Lurestan Province, SW Iran in the Zagros Orogen. On the basis of our new field, geochronology, and Hf isotopic data, combined with those from published literature, we might be able to test two hypotheses outlined below in order to highlight the possible key events of the Neo-Tethyan amalgamation history (Figs. 9, 10).

Hypothesis A Using a previously published scenario (Agard et al. 2005, 2011; Whitechurch et al. 2013; Wrobel-Daveau et al. 2010), Hypothesis A is proposed with three main periods (Fig. 11). The predominance of 65–300 Ma zircons in samples A29 and A30 fits with regional-scale obduction of the Neo-Tethyan oceanic lithosphere at ca. 100–65 Ma onto Arabia, which is similar to timing of emplacement of the Semail ophiolite in Oman (Saura et al. 2015; Searle and Cox 1999). Based on the ocean island-arc signature of the Harsin ophiolite, obduction of the Neo-Tethyan lithosphere during Late Cretaceous time is suggested to have developed from the volcanic arc (Agard et al. 2005). Formation of the ETMD could be triggered by slab break-off and the melting of the metasomatized subcontinental lithosphere in the Early Paleocene (Agard et al. 2011; Chiu et al. 2013; Verdel et al. 2011; Whitechurch et al. 2013). Meanwhile, erosion of obducted ophiolite and abundant early to middle Triassic volcanism fed the detrital basins forming the shallowing upwards Amiran–Taleh Zang–Kashkan detrital succession (Homke et al. 2009; Saura et al. 2011). Continued subduction of the remnant oceanic crust then led to closure of the Neo-Tethys Ocean. After strong and long weathering and erosion, the limited remnants of the obducted ophiolite were not able to supply appreciable detritus to the Gachsaran and Agha Jari Formations. In contrast, abundant zircons from the ETMD and SSZ were transported into the basin and deposited after collision between Arabia and Eurasia. Based on the provenance analysis of the sediments, the initial continental collision of Arabia and Eurasia plates is suggested to have occurred before 18 Ma, the depositional age of sample A28. This inference is also consistent with petrographic and thermochronological studies in the Fars Province, which indicates that the collision is constrained to be no younger than 19.7 Ma (Khadivi et al. 2012). This age is the depositional age of the base of the Razak Formation, the lateral equivalent of the evaporitic Gachsaran Formation (Khadivi et al. 2012). The age pattern for sample A25 probably suggests a strong Arabian basement source that was entering the foreland basin at ca. 5 Ma.

Hypothesis B Hypothesis B is developed from Farhoudi (1978) (Fig. 12), which using present arc models (Makran Arc System) suggests a new trench was located at the margin of the Persian Gulf in the Fars province. The Late Permian–Triassic opening of Neo-Tethys separated the Cimmerian continent from Gondwanaland with abundant Early-Middle Triassic volcanism. This was followed by the amalgamation and/or welding together of oceanic crust to Triassic volcanic rocks, during Late Cretaceous intra-ocean

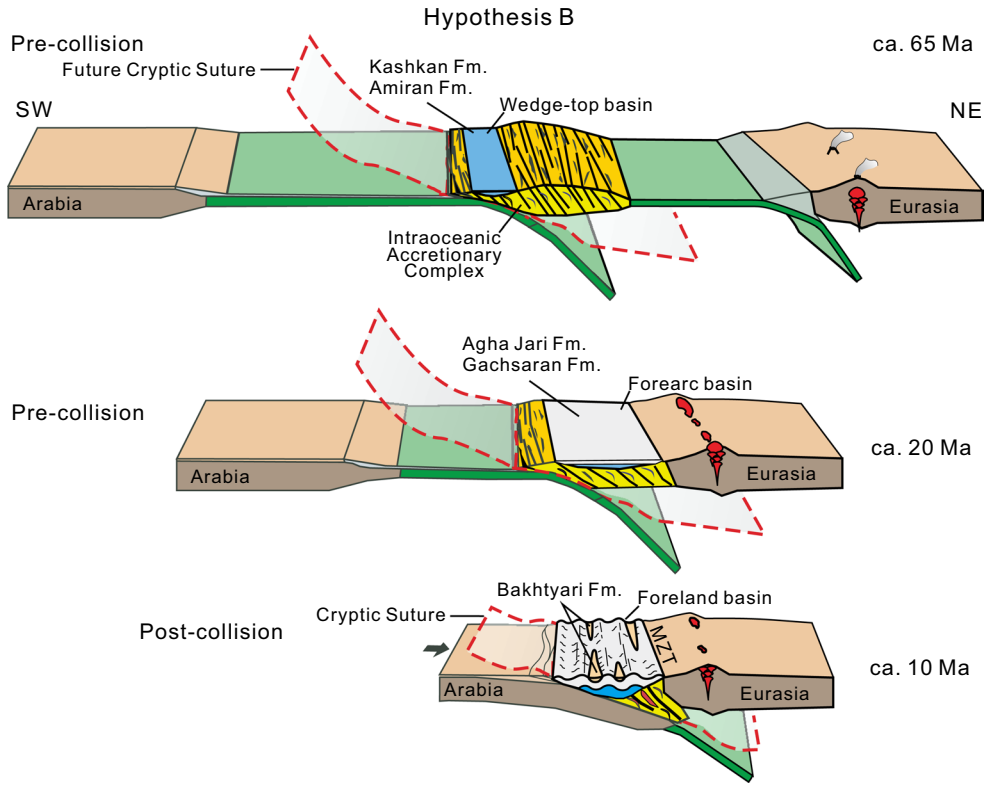

Fig. 12 Simplified tectonic evolution model (Hypothesis B) showing the amalgamation history of Neo-Tethys since Paleocene. Basin type changed (as indicated) during each period of the tectonic evolution shown. See text for details

subduction forming the Neo-Tethyan ophiolitic accretionary complex. In Paleocene–Eocene time this complex was the source for sediment supplied to the wedge-top basin. The lithospheric-scale reconstruction for this event is similar to that proposed in Hypothesis A except for the different locations of the Amiran–Taleh Zang–Kashkan detrital successions. An intra-ocean accretionary complex and its overlying sediments started to collide with Eurasia in the Early Miocene. This might have led to a tectonic setting similar to the present-day accretionary prisms in the Makran area. The trench slope break migrated oceanward to the new trench along with continued subduction of the remnant oceanic crust, which then led to closure of the Neo-Tethys ocean. In Hypothesis B, samples A26–A30 are characterized by a transition from the northern Neo-Tethyan ophiolitic accretionary complex or Eurasian domains and carry obviously no inputs from the southerly Arabian plate. Although Pan-African sources are also observed in the detrital age populations of samples A26, A27 and A28, according to the paleocurrent direction information these old zircons were probably sourced from Iran reflecting the East African Orogen (Horton et al. 2008). Therefore, we propose that the initial continental collision of the Arabia and Eurasia plates was post 11.2 Ma (the depositional age of sample A26). While the provenance of sample A25 was most likely derived from Arabia because of its distinctly similar age distribution pattern with contributions from Eurasia. So, we conclude that sample A25 located on the Zagros foreland basin represents post-collisional sediments with mixed provenance. This finding implies that the Arabia–Eurasia continental collision was pre-5 Ma, i.e., the depositional age of sample A25. Therefore, in this hypothesis, the initial continental collision between Arabia and Eurasia most likely occurred in SW Iran at some time between 11.2 and 5 Ma. This significantly younger age is similar to that proposed by Talebian and Jackson (2004) and is represented by the regional angular unconformity between the Agha Jari and Bakhtyari Formations, which was previously considered to date the peak time of orogeny in the Zagros (Hessami et al. 2001). Furthermore, we recognize that the MZT is the boundary between the accretionary complex and Eurasia. Accordingly, the actual suture (trench) in Hypothesis B could be located at the SW margin of the Lurestan province and buried under Quaternary desert sand. Therefore, the Cryptic Suture is a 'plane' separating Eurasian accretionary units from Arabian basement, representing termination of the consumed ocean (Fig. 12). That means not all ophiolites represent the exact places of the suture, and the suture position may lay on the bottom of the accretionary complex. As Dewey et al. (1986)

remarked, the recognition and understanding of continental collision depend upon our ability to recognize and understand collisional sutures, whose position is not always readily apparent, sutures may be exceedingly cryptic.

Our data could at first glance be reconciled with either of the two alternative hypotheses, each of which implies a different amalgamation history for the Neo-Tethys. However, only a few Pan-African sources and pre-Neoproterozoic signatures are observed in the detrital age populations of samples A26–A30. The age distribution pattern of these samples therefore differs markedly from that of Arabian samples. Also some blocks in the Neo-Tethys were rifted from southerly Gondwana and joined Eurasia in the Mesozoic, such as Cimmerian continent, which may have carried some Pan-African sources and/or pre-Neoproterozoic signatures. Therefore, for a Cenozoic collision event, minor Pan-African sources and/or pre-Neoproterozoic signatures would not be necessarily a diagnostic criterion for the source from Arabia, in particular when they are minor. Furthermore, only the youngest sample A25 is dominated by zircons showing a Pan-African signature together with minor input from Eurasia. These facts are, however, inconsistent with Hypothesis A, in which Arabian-Nubian Shield should have consistently contributed considerable zircons to all overlying Cenozoic deposits since 18 Ma, which is not the case.

Although we can assume that, the reason why these samples have so few old zircons could be that Arabia became a vast low-relief surface and could not provide sufficient material following strong and long weathering and erosion. The fact is that the upper Permian to Cenozoic succession in Arabia thickens eastward to more than 8 km, reflecting continuous subsidence of the Arabian passive margin facing Neo-Tethys (Garzanti et al. 2013). As Arabia remained as a stable platform during this period, this suggests that quartz and feldspar as well as heavy minerals could have been transported to coastal areas. To be compatible with this observation a remnant ocean separating Arabia from the basins containing the Kashkan and Amiram Formations is therefore proposed in Hypothesis B, a multiple extensional tectonic scenario which has been compatible with an intra-oceanic metamorphic complex from 79 to 36 Ma (Ao et al. 2016, in press). Meanwhile, subduction of the remnant oceanic crust led to closure of the Neo-Tethys Ocean. Then the continued post-collisional underthrusting of the Arabian basement is suggested as a mechanism for generating shallow earthquakes by the outward migration of the trench slope break (Farhoudi 1978), because continental crust is less dense than oceanic crust. This suggestion is supported by the focal mechanism of earthquakes recently observed along the Zagros Orogen (Nissen et al. 2011; Nowroozi 1976; Talebian and Jackson 2004). Further, the thickness of the Bakhtyari Molasse increases rapidly from a few meters to 2500 m southwestwards to the northeastern edge of the Mesopotamian Depression, which was suggested by Bird et al. (1975) to be the site of continental underthrusting. Finally, the most direct evidence supporting Hypothesis B is that it fits well with geological observation, for instance, most asymmetric folds in the ZFTB display steeper SW limbs (Talebian and Jackson 2004), sediments in the ZFTB becoming progressively younger from northeast to southwest (Saura et al. 2015). From the foregoing we conclude that Hypothesis B is our preferred tectonic scenario.

Acknowledgments This work was supported by the "Strategic Priority Research Program (B)" of the Chinese Academy of Sciences (XDB03010801), National Natural Science Foundation of China (41190072, 41230207, 41302167 and 41472192), and China Postdoctoral Council (20100480452, 2012T50135 and International Postdoctoral Exchange Fellowship). We thank B. P. Kohn, B. F. Windley, S. Glorie, and J. Gillespie for constructive discussion and language polishing. Special thanks are expressed to the guest editor and reviewers for their critical comments that promoted substantial improvements in this manuscript.

References

Agard P, Omrani J, Jolivet L, Mouthereau F (2005) Convergence history across Zagros (Iran): constraints from collisional and earlier deformation. Int J Earth Sci 94:401–419

Agard P, Omrani J, Jolivet L, Whitechurch H, Vrielynck B, Spakman W, Monie P, Meyer B, Wortel R (2011) Zagros orogeny: a subduction-dominated process. Geol Mag 148:692–725

Ahadnejad V, Valizadeh MV, Deevsalar R, Rezaei-Kahkhaei M (2011) Age and geotectonic position of the Malayer granitoids: implication for plutonism in the Sanandaj-Sirjan Zone, W Iran. Neues Jahrb Geol Palaontol Abh 261:61–75

Ahmadi Khalaji A, Esmaeily D, Valizadeh MV, Rahimpour-Bonab H (2007) Petrology and geochemistry of the granitoid complex of Boroujerd, Sanandaj-Sirjan Zone, Western Iran. J Asian Earth Sci 29:859–877

Alavi M (1994) Tectonics of the zagros orogenic belt of Iran: new data and interpretations. Tectonophysics 229:211–238

Allen MB, Armstrong HA (2008) Arabia–Eurasia collision and the forcing of mid-Cenozoic global cooling. Paleogeogr Paleoclimatol Paleoecol 265:52–58

Andersen T (2002) Correction of common lead in U–Pb analyses that do not report 204Pb. Chem Geol 192:59–79

Ao SJ, Xiao WJ, Khalatbari Jafari M, Talebian M, Chen L, Wan B, Ji WQ, Zhang ZY (2016) U–Pb zircon ages, field geology and geochemistry of the Kermanshah ophiolite (Iran): from continental rifting at 79 Ma to oceanic core complex at ca. 36 Ma in the southern Neo-Tethys. Gondwana Res. doi:10.1016/j.gr.2015.1001.1014

ArRajehi A, McClusky S, Reilinger R, Daoud M, Alchalbi A, Ergintav S, Gomez F, Sholan J, Bou-Rabee F, Ogubazghi G, Haileab B, Fisseha S, Asfaw L, Mahmoud S, Rayan A, Bendik R, Kogan L (2010) Geodetic constraints on present-day motion of the Arabian Plate: implications for Red Sea and Gulf of Aden rifting. Tectonics 29:TC3011. doi:10.1029/2009TC002482

Austermann J, Iaffaldano G (2013) The role of the Zagros orogeny in slowing down Arabia–Eurasia convergence since ~5 Ma. Tectonics 32:351–363

Azizi H, Asahara Y, Mehrabi B, Chung SL (2011a) Geochronological and geochemical constraints on the petrogenesis of high-K granite from the Suffi abad area, Sanandaj-Sirjan Zone, NW Iran. Chem Erde Geochem 71:363–376

Azizi H, Tanaka T, Asahara Y, Chung SL, Zarrinkoub MH (2011b) Discrimination of the age and tectonic setting for magmatic rocks along the Zagros thrust zone, northwest Iran, using the zircon U–Pb age and Sr–Nd isotopes. J Geodyn 52:304–320

Bagheri S, Stampfli GM (2008) The Anarak, Jandaq and Posht-e-Badam metamorphic complexes in central Iran: New geological data, relationships and tectonic implications. Tectonophysics 451:123–155

Ballato P, Uba CE, Landgraf A, Strecker MR, Sudo M, Stockli DF, Friedrich A, Tabatabaei SH (2011) Arabia–Eurasia continental collision: insights from late Tertiary foreland-basin evolution in the Alborz Mountains, northern Iran. Geol Soc Am Bull 123:106–131

Berberian M, King GCP (1981) Towards a paleogeography and tectonic evolution of Iran. Can J Earth Sci 18:210–265

Bird P, Toksöz MN, Sleep NH (1975) Thermal and mechanical models of continent–continent convergence zones. J Geophys Res 80:4405–4416

Carter A, Najman Y, Bahroudi A, Bown P, Garzanti E, Lawrence RD (2010) Locating earliest records of orogenesis in western Himalaya: evidence from Paleogene sediments in the Iranian Makran region and Pakistan Katawaz basin. Geology 38:807–810

Cawood PA, Nemchin AA, Leverenz A, Saeed A, Balance PF (1999) U/Pb dating of detrital zircons: implications for the provenance record of Gondwana margin terranes. Geol Soc Am Bull 111:1107–1119

Cawood PA, Wang YJ, Xu YJ, Zhao GC (2013) Locating South China in Rodinia and Gondwana: a fragment of greater India lithosphere? Geology 41:903–906

Chiu HY (2013) The Neotethyan subduction and Zagros orogeny: constraints from zircon U–Pb age and Hf isotopic study of magmatic rocks from Iran. Dissertation, National Taiwan University

Chiu HY, Chung SL, Zarrinkoub MH, Mohammadi SS, Khatib MM, Iizuka Y (2013) Zircon U–Pb age constraints from Iran on the magmatic evolution related to Neotethyan subduction and Zagros orogeny. Lithos 162–163:70–87

Delaloye M, Desmons J (1980) Ophiolites and melange terranes in Iran: a geochronological study and its paleotectonic implications. Tectonophysics 68:83–111

Dercourt J, Zonenshain LP, Ricou LE, Kazmin VG, Le Pichon X, Knipper AL, Grandjacquet C, Sbortshikov IM, Geyssant J, Lepvrier C, Pechersky DH, Boulin J, Sibuet JC, Savostin LA, Sorokhtin O, Westphal M, Bazhenov ML, Lauer JP, Biju-Duval B (1986) Geological evolution of the tethys belt from the atlantic to the pamirs since the LIAS. Tectonophysics 123:241–315

Dewey JF, Pitman WC, Ryan WBF, Bonnin J (1973) Plate tectonics and the evolution of the alpine system. Geol Soc Am Bull 84:3137–3180

Dewey JF, Hempton MR, Kidd WSF, Saroglu F, Şengör AMC (1986) Shortening of continental lithosphere: the neotectonics of Eastern Anatolia—a young collision zone. Geol Soc Lond Spec Publ 19:1–36

Ehrenberg SN, Pickard NAH, Laursen GV, Monibi S, Mossadegh ZK, Svana TA, Aqrawi AAM, McArthur JM, Thirlwall MF (2007) Strontium isotope stratigraphy of the Asmari Formation (Oligocene–Lower-Miocene), SW Iran. J Pet Geol 30:107–128

Emami H (2008) Foreland propagation folding and structure of the Mountain Front Flexure in the Pusht-e Kuh arc (NW Zagros, Iran). Dissertation, University of Barcelona

Esna-Ashari A, Tiepolo M, Valizadeh M-V, Hassanzadeh J, Sepahi A-A (2012) Geochemistry and zircon U–Pb geochronology of Aligoodarz granitoid complex, Sanandaj-Sirjan Zone. Iran. J Asian Earth Sci 43:11–22

Fakhari MD, Axen GJ, Horton BK, Hassanzadeh J, Amini A (2008) Revised age of proximal deposits in the Zagros foreland basin and implications for Cenozoic evolution of the High Zagros. Tectonophysics 451:170–185

Farhoudi G (1978) A comparison of Zagros geology to island arcs. J Geol 86:323–334

Garzanti E, Vermeesch P, Andò S, Vezzoli G, Valagussa M, Allen K, Kadi KA, Al-Juboury AIA (2013) Provenance and recycling of Arabian desert sand. Earth Sci Rev 120:1–19

Gavillot Y, Axen GJ, Stockli DF, Horton BK, Fakhari MD (2010) Timing of thrust activity in the High Zagros fold-thrust belt, Iran, from (U–Th)/He thermochronometry. Tectonics 29:TC4025. doi: 10.1029/2009TC002484

Gehrels G (2014) Detrital zircon U–Pb geochronology applied to tectonics. Annu Rev Earth Planet Sci 42:127–149

Ghazi AM, Hassanipak AA (1999) Geochemistry of subalkaline and alkaline extrusives from the Kermanshah ophiolite, Zagros Suture Zone, Western Iran: implications for Tethyan plate tectonics. J Asian Earth Sci 17:319–332

Gradstein FM, Ogg JG, Schmitz M, Ogg G (2012) The geologic time scale 2012 2-volume set. Elsevier, Amsterdam

Hempton MR (1987) Constraints on Arabian Plate motion and extensional history of the Red Sea. Tectonics 6:687–705

Hessami K, Koyi HA, Talbot CJ, Tabasi H, Shabanian E (2001) Progressive unconformities within an evolving foreland fold-thrust belt, Zagros Mountains. J Geol Soc 158:969–981

Homke S, Vergés J, Garcés M, Emami H, Karpuz R (2004) Magnetostratigraphy of Miocene–Pliocene Zagros foreland deposits in the front of the Push-e Kush Arc (Lurestan Province, Iran). Earth Planet Sci Lett 225:397–410

Homke S, Verges J, Serra-Kiel J, Bernaola G, Sharp I, Garces M, Montero-Verdu I, Karpuz R, Goodarzi MH (2009) Late Cretaceous–Paleocene formation of the proto-Zagros foreland basin, Lurestan Province, SW Iran. Geol Soc Am Bull 121:963–978

Horton BK, Hassanzadeh J, Stockli DF, Axen GJ, Gillis RJ, Guest B, Amini A, Fakhari MD, Zamanzadeh SM, Grove M (2008) Detrital zircon provenance of Neoproterozoic to Cenozoic deposits in Iran: implications for chronostratigraphy and collisional tectonics. Tectonophysics 451:97–122

Hunziker D, Burg J-P, Bouilhol P, von Quadt A (2015) Jurassic rifting at the Eurasian Tethys margin: geochemical and geochronological constraints from granitoids of North Makran, southeastern Iran. Tectonics 34:571–593

James GA, Wynd JG (1965) Stratigraphic nomenclature of Iranian Oil Consortium Agreement Area. AAPG Bull 49:2182–2245

Khadivi S, Mouthereau F, Barbarand J, Adatte T, Lacombe O (2012) Constraints on palaeodrainage evolution induced by uplift and exhumation on the southern flank of the Zagros-Iranian Plateau. J Geol Soc 169:83–97

Mahmoudi S, Corfu F, Masoudi F, Mehrabi B, Mohajjel M (2011) U–Pb dating and emplacement history of granitoid plutons in the northern Sanandaj-Sirjan Zone, Iran. J Asian Earth Sci 41:238–249

McQuarrie N, van Hinsbergen DJJ (2013) Retrodeforming the Arabia–Eurasia collision zone: age of collision versus magnitude of continental subduction. Geology 41:315–318

Moghadam HS, Corfu F, Stern RJ (2013) U–Pb zircon ages of Late Cretaceous Nain-Dehshir ophiolites, central Iran. J Geol Soc 170:175–184

Mohajjel M, Fergusson CL, Sahandi MR (2003) Cretaceous-Tertiary convergence and continental collision, Sanandaj-Sirjan Zone, western Iran. J Asian Earth Sci 21:397–412

Morag N, Avigad D, Gerdes A, Belousova E, Harlavan Y (2011) Detrital zircon Hf isotopic composition indicates long-distance transport of North Gondwana Cambrian-Ordovician sandstones. Geology 39:955–958

Mouthereau F, Lacombe O, Verges J (2012) Building the Zagros collisional orogen: timing, strain distribution and the dynamics of Arabia/Eurasia plate convergence. Tectonophysics 532:27–60

Nissen E, Tatar M, Jackson JA, Allen MB (2011) New views on earthquake faulting in the Zagros fold-and-thrust belt of Iran. Geophys J Int 186:928–944

Nowroozi AA (1976) Seismotectonic provinces of Iran. Bull Seismol Soc Am 66:1249–1276

Saura E, Verges J, Homke S, Blanc E, Serra-Kiel J, Bernaola G, Casciello E, Fernandez N, Romaire I, Casini G, Embry JC, Sharp IR, Hunt DW (2011) Basin architecture and growth folding of the NW Zagros early foreland basin during the Late Cretaceous and early Tertiary. J Geol Soc 168:235–250

Saura E, Garcia-Castellanos D, Casciello E, Parravano V, Urruela A, Verges J (2015) Modeling the flexural evolution of the Amiran and Mesopotamian foreland basins of NW Zagros (Iran–Iraq). Tectonics 34:377–395

Searle M, Cox J (1999) Tectonic setting, origin, and obduction of the Oman ophiolite. Geol Soc Am Bull 111:104–122

Şengör AMC, Natal'in BA (1996) Paleotectonics of Asia: fragments of a synthesis. In: Yin A, Harrison M (eds) The tectonic evolution of Asia. Cambridge University Press, Cambridge, pp 486–641

Şengör AMC, Altıner D, Cin A, Ustaömer T, Hsü KJ (1988) Origin and assembly of the Tethyside orogenic collage at the expense of Gondwana Land. Geol Soc Lond Spec Publ 37:119–181

Shahbazi H, Siebel W, Pourmoafee M, Ghorbani M, Sepahi AA, Shang CK, Vousoughi Abedini M (2010) Geochemistry and U–Pb zircon geochronology of the Alvand plutonic complex in Sanandaj-Sirjan Zone (Iran): new evidence for Jurassic magmatism. J Asian Earth Sci 39:668–683

Stampfli GM, Borel GD (2002) A plate tectonic model for the Paleozoic and Mesozoic constrained by dynamic plate boundaries and restored synthetic oceanic isochrons. Earth Planet Sci Lett 196:17–33

Stoneley R (1981) The geology of the Kuh-e Dalneshin area of southern Iran, and its bearing on the evolution of southern Tethys. J Geol Soc 138:509–526

Talebian M, Jackson J (2004) A reappraisal of earthquake focal mechanisms and active shortening in the Zagros mountains of Iran. Geophys J Int 156:506–526

Verdel C, Wernicke BP, Hassanzadeh J, Guest B (2011) A Paleogene extensional arc flare-up in Iran. Tectonics 30:TC3008. doi:10.1029/2010TC002809

Vermeesch P (2012) On the visualisation of detrital age distributions. Chem Geol 312–313:190–194

Whitechurch H, Omrani J, Agard P, Humbert F, Montigny R, Jolivet L (2013) Evidence for Paleocene–Eocene evolution of the foot of the Eurasian margin (Kermanshah ophiolite, SW Iran) from back-arc to arc: implications for regional geodynamics and obduction. Lithos 182–183:11–32

Woodhead JD, Hergt JM (2005) A preliminary appraisal of seven natural zircon reference materials for in situ Hf isotope determination. Geostand Geoanal Res 29:183–195

Wrobel-Daveau JC, Ringenbach JC, Tavakoli S, Ruiz GMH, Masse P, de Lamotte DF (2010) Evidence for mantle exhumation along the Arabian margin in the Zagros (Kermanshah area, Iran). Arab J Geosci 3:499–513

Wu FY, Yang YH, Xie LW, Yang JH, Xu P (2006) Hf isotopic compositions of the standard zircons and baddeleyites used in U–Pb geochronology. Chem Geol 234:105–126

Wu FY, Ji WQ, Liu CZ, Chung SL (2010) Detrital zircon U–Pb and Hf isotopic data from the Xigaze fore-arc basin: constraints on Transhimalayan magmatic evolution in southern Tibet. Chem Geol 271:13–25

Yin A (2010) Cenozoic tectonic evolution of Asia: a preliminary synthesis. Tectonophysics 488:293–325